

Interatomic distance dependence of resonant energy-transfer phenomena

F. Grüll, A. B. Voitkiv, and C. Müller

Institut für Theoretische Physik I, Heinrich Heine Universität Düsseldorf, Universitätsstr. 1, 40225 Düsseldorf, Germany

(Dated: July 28, 2021)

It is well known that interatomic or intermolecular interactions driven by two-center electronic dipole-dipole correlations fall off rapidly with the inter-site distance. We show, however, that the effective strength of interatomic reaction channels, which are triggered by a resonant field, can exhibit a nonmonotonous distance dependence, being strongly reduced when the atoms come closer. This surprising result is demonstrated by considering resonant two-center photoionization as an example. Our findings are supported by available experimental data.

Introduction—Interatomic and intermolecular processes are under very active scrutiny in recent years. The research area has been strongly triggered by the prediction of interatomic Coulombic decay (ICD) where electronic excitation energy of an atom is transferred radiationlessly to a neighbor atom resulting in its ionization [1–3]. ICD is of particular importance, when a single-center Auger decay is energetically forbidden, and can proceed much faster than radiative decay. It has first been observed in noble gas dimers and clusters [4, 5]. Corresponding measurements rely on advanced experimental techniques, such as third-generation synchrotron sources and few-body coincidence spectrometers [6].

Similar interatomic energy-transfer processes are known in various areas of physics, comprising exciton dynamics in solids [7], quantum optical ensembles and cold Rydberg gases [8]. They also play an important role in chemistry and biology, as exemplified by ICD in water [9] and hydrated biomolecules [10], lattice dynamics in polymers [11], and Förster resonances in chromophores [12]. Slow electrons set free via ICD cascades are of great relevance for applied radiation biology [13]. It has thus been concluded that interatomic energy-transfer reactions are ubiquitous in nature.

In most of the cases, the interatomic coupling arises from the long-range interaction between two dipoles. It is of the form (in atomic units)

$$\hat{V}_{ee} = \frac{\mathbf{r} \cdot \boldsymbol{\xi}}{R^3} - \frac{3(\mathbf{r} \cdot \mathbf{R})(\boldsymbol{\xi} \cdot \mathbf{R})}{R^5}, \quad (1)$$

with the internuclear separation \mathbf{R} and the coordinates of the active electrons \mathbf{r} and $\mathbf{r}' = \mathbf{R} + \boldsymbol{\xi}$. The generic R^{-3} scaling is modified when retardation effects or non-dipole transitions are considered. Yet always the interaction quickly falls off when the interatomic distance grows. Accordingly, inter-site energy transfers are expected to be the more efficient, the closer the atoms lie together.

An interatomic process involving ICD is two-center resonant photoionization (2CPI) in a heteroatomic system of two atoms, say A and B [14–18]. Here, a neighboring atom B is first resonantly excited by photoabsorption, this way creating an autoionizing state of the two-center system, which afterwards stabilizes via ICD. The original theory [14, 15] assumed, for simplicity, two spatially

well-separated atoms with fixed distance vector \mathbf{R} . Since the photoabsorption step is included in the treatment, a comparison with the direct photoionization of atom A is feasible. Application to Li as atom A and He as atom B at an interatomic distance of 10 \AA as an example, a relative enhancement of 2CPI over the direct photoionization of Li by a factor $\simeq 10^6$ is predicted.

2CPI was experimentally observed in NeHe dimers [19–21]. Up to a $\simeq 100$ -fold relative enhancement was found, which is very substantial, though much smaller than the enormous amplification predicted for the LiHe model system. This discrepancy appears astonishing in light of the fact that the internuclear separation in the NeHe ground state is substantially less than in LiHe lying between $\approx 2.5\text{--}6 \text{ \AA}$ [22]. Accordingly, ICD proceeds much faster in NeHe than in LiHe, occurring on a timescale of hundreds of femtoseconds. A considerable enhancement of photoionization due to 2CPI has very recently also been seen in ArNe clusters [23], but again at much lower scale than in LiHe.

The reasons for so vastly different (and counterintuitive) levels of enhancement have not been clarified yet, nor has a theoretical explanation for the observed levels been given. It is suggestive to assume that the differences between the measurements and the original theory result from the molecular structure of the target systems which was not taken into account there. In fact, ICD in NeHe and other noble-gas dimers is known to be very sensitive to the vibrational nuclear motion [22, 24].

However, as we show in this paper, the difference between the relative enhancement predicted in LiHe versus the one observed in NeHe is not caused by the molecular structure of a dimer in the first place. The reduction in 2CPI efficiency rather occurs because the Ne and He atoms are *so close* to each other. This result stands in sharp contrast to the intuitive expectation that close distances should generally facilitate interatomic energy transfer processes [see Eq. (1)]. Nevertheless, it can be obtained within a relatively simple theoretical treatment of the 2CPI process in a weakly bound dimer, which explains why, close to the resonance, a large ICD rate can have a detrimental impact on the effectiveness of 2CPI.

Theoretical description—We consider a system of two atoms, A and B , which are initially in their ground states.

They are separated by a sufficiently large distance R (covering at least several \AA), such that their individuality is basically preserved, and exposed to a resonant electromagnetic field of the form

$$\mathbf{F}(t) = F_0 \cos(\omega t) \mathbf{e}_z \quad (2)$$

which is taken in the dipole approximation. Here, ω is the angular frequency and F_0 the field amplitude.

To start with, we assume the atoms to be at rest and take the position of the nucleus of atom A as the origin and denote the coordinates of the nucleus of atom B , the (active) electron of atom A and that of atom B by \mathbf{R} , \mathbf{r} and $\mathbf{r}' = \mathbf{R} + \boldsymbol{\xi}$, respectively, where $\boldsymbol{\xi}$ is the position of the electron of atom B with respect to its nucleus. Let atom B have an excited state χ_e reachable from the ground state χ_g by a dipole-allowed transition.

The total Hamiltonian describing the two atoms in the external electromagnetic field reads

$$\hat{H} = \hat{H}_0 + \hat{V}_{ee} + \hat{W}, \quad (3)$$

where \hat{H}_0 is the sum of the Hamiltonians for the noninteracting atoms A and B , and \hat{V}_{ee} the interaction between the atoms. $\hat{W} = \hat{W}_A + \hat{W}_B = \mathbf{F}(t) \cdot (\mathbf{r} + \mathbf{r}')$ denotes the interaction of the atoms with the electromagnetic field in the length gauge. It is assumed that $\omega_{ge}R/c \ll 1$, where ω_{ge} is the atomic transition frequency and c the speed of light, such that retardation effects can be neglected.

In the 2CPI process one has essentially three different basic two-electron configurations, which are schematically illustrated in Fig. 1: (I) $\Phi_i = \varphi_g(\mathbf{r})\chi_g(\boldsymbol{\xi})$ with total energy $E_i = \varepsilon_g + \varepsilon_g$, where both atoms are in the corresponding ground states φ_g and χ_g ; (II) $\Phi_a = \varphi_g(\mathbf{r})\chi_e(\boldsymbol{\xi})$ with total energy $E_a = \varepsilon_g + \varepsilon_e$, in which atom A is in the ground state while atom B is in the excited state χ_e ; (III) $\Phi_f = \varphi_p(\mathbf{r})\chi_g(\boldsymbol{\xi})$ with total energy $E_f = \varepsilon_p + \varepsilon_g$, where

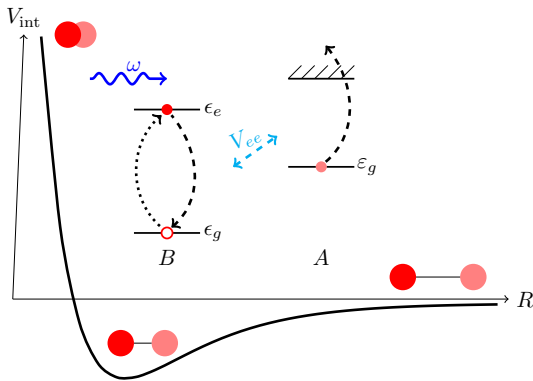


FIG. 1: Scheme of two-center resonant photoionization (2CPI), embedded in a generic potential curve $V_{\text{int}}(R)$ of a van-der-Waals dimer A - B . First, atom B is resonantly photoexcited; its subsequent decay by ICD leads to ionization of atom A via an interatomic dipole-dipole interaction V_{ee} . The shape of the potential curve determines at which internuclear distance R the process mostly occurs.

the electron of atom A has been emitted into the continuum with asymptotic momentum \mathbf{p} , while the electron of atom B has returned to the ground state.

Within the second order of time-dependent perturbation theory, the probability amplitude for 2CPI can be written as

$$S_{\mathbf{p}}^{(2)} = - \int_{-\infty}^{\infty} dt \langle \Phi_f | \hat{V}_{ee} | \Phi_a \rangle e^{-i(E_a - E_f)t} \times \int_{-\infty}^t dt' \langle \Phi_a | \hat{W}_B | \Phi_i \rangle e^{-i(E_i - E_a)t'} \quad (4)$$

Performing the time integrations, we obtain

$$S_{\mathbf{p}}^{(2)} = -i\pi \langle \varphi_{\mathbf{p}} | \mathbf{r} | \varphi_g \rangle \cdot \left(\mathbf{e}_z - \frac{3R_z}{R^2} \mathbf{R} \right) \times \frac{F_0}{R^3} \frac{|\langle \chi_e | \xi_z | \chi_g \rangle|^2}{\Delta + \frac{i}{2}\Gamma} \delta(\varepsilon_p - \varepsilon_0 - \omega), \quad (5)$$

where the detuning from the resonance $\Delta = \varepsilon_g + \omega - \varepsilon_e$ has been introduced and the total width $\Gamma = \Gamma_r + \Gamma_a$ of the excited state χ_e in atom B inserted. It accounts for the finite lifetime of this state and consists of the radiative width Γ_r and the two-center Auger (ICD) width Γ_a [25]. The delta function in Eq. (5) displays the law of energy conservation in the process.

From the transition amplitude we can obtain the total ionization cross section in the usual way by taking the absolute square, integrating it over the photoelectron momentum, and dividing it by the interaction time τ and the incident flux $j = \frac{cF_0^2}{8\pi\omega}$, that is

$$\sigma_{\text{at}}^{(2)}(R) = \frac{1}{j\tau} \int \frac{d^3p}{(2\pi)^3} \left| S_{\mathbf{p}}^{(2)} \right|^2 = \int d\Omega_p |\langle \varphi_{\mathbf{p}} | \mathbf{r} | \varphi_g \rangle \cdot (\mathbf{e}_z - 3 \cos \theta_R \mathbf{e}_R)|^2 \times \frac{\omega p}{2\pi c R^6} \frac{|\langle \chi_e | \xi_z | \chi_g \rangle|^4}{\Delta^2 + \frac{1}{4}\Gamma^2} \quad (6)$$

Here, the value of p is fixed by the energy conservation and we have introduced the unit vector $\mathbf{e}_R = \mathbf{R}/R$ along the internuclear separation and the angle θ_R between \mathbf{R} and the field direction [26]. Equation (6) can be rewritten using the cross section $\sigma_A^{(1)} = \int d\Omega_p |\langle \varphi_{\mathbf{p}} | z | \varphi_g \rangle|^2 \frac{\omega p}{2\pi c}$ for the direct photoionization of atom A by the electromagnetic field. For the special cases, when the separation vector \mathbf{R} between the atoms A and B is oriented either along the field direction or perpendicular to it, we obtain

$$\sigma_{\text{at}}^{(2)}(R) = \frac{\alpha}{R^6} \frac{|\langle \chi_e | \xi_z | \chi_g \rangle|^4}{\Delta^2 + \frac{1}{4}\Gamma^2} \sigma_A^{(1)} = \left(\frac{3\alpha c^3}{4\omega_{ge}^3 R^3} \right)^2 \frac{\Gamma_{r,ge}^2}{\Delta^2 + \frac{1}{4}\Gamma^2} \sigma_A^{(1)} \quad (7)$$

where $\alpha = 2$ for $\mathbf{R} \parallel \mathbf{F}_0$ and $\alpha = 1$ for $\mathbf{R} \perp \mathbf{F}_0$. In the second step, the dipole matrix element has been expressed by the corresponding radiative width $\Gamma_{r,ge} =$

$\frac{4\omega_{ge}^3}{3c^3} |\langle \chi_e | \xi_z | \chi_g \rangle|^2$ with $\omega_{ge} = \epsilon_e - \epsilon_g$. The compact formula (7) applies to two individual atoms at a distance R , carrying a single active electron each.

Below we will consider diatomic systems containing helium as atom B . In this case, the two equivalent electrons must be described by appropriately symmetrized wave functions and their interaction with the field by a two-particle extension of the operator \hat{W}_B . This leads to an additional factor of 4 in the 2CPI cross section [18]. Taking this into account and assuming that the field is exactly resonant ($\Delta = 0$), the ratio of the 2CPI and direct photoionization cross sections becomes

$$\frac{\sigma_{\text{at}}^{(2)}(R)}{\sigma_A^{(1)}} = \left(\frac{3\alpha c^3}{\omega^3 R^3} \right)^2 \frac{\Gamma_{r,ge}^2}{(\Gamma_r + \Gamma_a)^2}. \quad (8)$$

By expressing the Auger width Γ_a according to

$$\Gamma_a(R) = \frac{3}{2\pi} \frac{c^4}{\omega^4 R^6} \Gamma_{r,ge} \sigma_A^{(1)} \quad (9)$$

(see, e.g., [27]), Eq. (7) can be put in a form which enables one a better understanding of the interatomic distance dependence of the 2CPI:

$$\sigma_{\text{at}}^{(2)}(R) = \frac{\alpha^2}{2} \sigma_B^{(\text{exc})} \frac{\Gamma_a \Gamma_{r,ge}}{(\Gamma_r + \Gamma_a)^2}, \quad (10)$$

where $\sigma_B^{(\text{exc})} = 3\pi c^2 / \omega^2$ [28] is the cross section for resonant photoexcitation of atom B .

Apart from a numerical prefactor of order unity, Eq. (10) can be represented as a product of two terms, $\sigma_B^{(\text{exc})} \Gamma_{r,ge} / (\Gamma_r + \Gamma_a)$ and $\Gamma_a / (\Gamma_r + \Gamma_a)$.

The first of them describes the photoexcitation step of 2CPI resulting in the creation of the intermediate state. Since $\Gamma_{r,ge} / (\Gamma_r + \Gamma_a) < \Gamma_{r,ge} / \Gamma_r$ it is seen that compared to an isolated atom B ($\Gamma_a = 0$) the probability for the resonant excitation in the A - B system is reduced due to a broadening of the resonance caused by the presence of the additional deexcitation pathway via ICD.

The second term, which is simply a branching ratio, determines the probability that afterwards the intermediate state decays via ICD. Unlike the first one, it increases with Γ_a approaching 1 at $\Gamma_a \gg \Gamma_r$.

At $\Gamma_{r,ge} \simeq \Gamma_r$ (which, in particular, holds for the systems studied below) the optimal enhancement of 2CPI over direct photoionization is reached for $\Gamma_a \approx \Gamma_r$, strongly decreasing both at $\Gamma_a \ll \Gamma_r$ and $\Gamma_a \gg \Gamma_r$. Since Γ_a falls with R , this suggests a nonmonotonous behavior of 2CPI on the dimer size: there is an 'optimal' value, where the efficiency of 2CPI is maximal and from where it decreases not only towards larger but also towards smaller sizes.

We now include effects of the nuclear motion in a weakly bound molecule. The Coulomb, exchange and van-der-Waals interactions between the atoms A and B

create a static potential $V_{\text{int}}(R)$, whose form depends on the electron configuration and in which the atomic nuclei occupy discrete vibrational levels. The wave functions of the system are accordingly amended, $\Psi_{i,a,f} = \Phi_{i,a,f}(\mathbf{r}, \boldsymbol{\xi}) \psi_{i,a,f}^{(\nu)}(R)$, to include the internuclear coordinate. When the derivation given above is repeated with these molecular states, the ratio of cross sections adopts the modified form [18]

$$\frac{\sigma_{\text{mol}}^{(2)}}{\sigma_{\text{mol}}^{(1)}} = \frac{\sigma_{\text{at}}^{(2)}(R_{\text{eq}})}{\sigma_A^{(1)}} \left(\frac{R_{\text{eq}}^3 \text{FC}_{i,a} \langle \psi_f^{(\nu_f)} | R^{-3} | \psi_a^{(\nu_a)} \rangle}{\text{FC}_{i,f}} \right)^2 \quad (11)$$

for a given set of vibrational quantum numbers ν_i , ν_a and ν_f . Here, the Franck-Condon factors

$$\text{FC}_{i,a} = \langle \psi_a^{(\nu_a)} | \psi_i^{(\nu_i)} \rangle = \int dR [\psi_a^{(\nu_a)}(R)]^* \psi_i^{(\nu_i)}(R) \quad (12)$$

and similarly for $\text{FC}_{i,f}$ have been introduced. The quadratic factor in Eq. (11), which accounts for the nuclear motion, will be referred to as F_{nuc} below. Note that it was made dimensionless by inserting the equilibrium distance R_{eq} between the nuclei into the formula.

The quantum number ν_a in Eq. (11) determines the vibrational nuclear wave function of the two-center autoionizing state and fixes the precise value of the associated resonant transition energy. The full expression for $\sigma_{\text{mol}}^{(2)}$ contains a coherent sum over the intermediate state and an incoherent sum over the final state quantum numbers, including ν_f [18].

Before proceeding further we note that the processes of 2CPI and direct photoionization are generally subject to quantum interference because they lead to the same final state (atom B merely serves as a catalyzer). However, for parameters where 2CPI strongly dominates, the interference is of minor importance and may be neglected.

Discussion—Based on Eqs. (8), (10) and (11) we can now compare the relative enhancement of 2CPI over direct photoionization in LiHe and NeHe dimers.

For a system of Li and He at $R = 10 \text{ \AA}$ considered as individual atoms, the ratio $\sigma_{\text{at}}^{(2)} / \sigma_A^{(1)}$ in Eq. (8) attains the value $\approx 4 \times 10^6$, assuming that the incident photon energy $\omega \approx 21.2 \text{ eV}$ is resonant to the $1s \rightarrow 2p$ transition in helium and taking $\alpha = 1$ for definiteness. In this scenario, the radiative width $\Gamma_r^{(2p)} = \Gamma_{r,ge}^{(2p)} \approx 1.18 \times 10^{-6} \text{ eV}$ [29] is much larger than the Auger width Γ_a . When a LiHe dimer [30] is considered instead, the single resonance splits into a multiplet of resonances, in accordance with the various vibrational transitions [18]. On each of these resonances, the nuclear motion tends to reduce the enhancement but not dramatically ($F_{\text{nuc}} \sim 0.1$ for favoured transitions $\nu_i \rightarrow \nu_a \rightarrow \nu_f$). Averaging over the molecular orientations with respect to the field, when the dimers are randomly distributed, leads to a further

reduction of the cross section by a geometrical factor of order unity.

In the experiment [19], Ne is ionized by synchrotron photons of energy $\omega \approx 23.1$ eV which corresponds to the $1s \rightarrow 3p$ transition in He (note that the $1s \rightarrow 2p$ transition energy lies below the ionization potential of Ne). The largest enhancement (by a factor of $\simeq 60$ –100, see [19, 20]) was observed when the intermediate state $1s3p\pi$ with $\nu_a = 2$ was populated. The Auger width Γ_a of this state can be estimated from the 'local' width (9) which applies to a fixed value of R , by taking an average over the probability density $|\psi_a^{(\nu_a)}(R)|^2$ of the vibrational state and, accordingly, amounts to $\Gamma_a \approx 1$ meV. This value agrees very well with the result of advanced quantum chemical calculations [20]. Γ_a turns out to be orders of magnitude larger than the radiative width $\Gamma_r^{(3p)} \approx 3.7 \times 10^{-7}$ eV [29], [31].

With these numbers, we obtain $\bar{\sigma}_{\text{mol}}^{(2)}/\sigma_{\text{mol}}^{(1)} \approx 320$, which is by 3–4 orders of magnitude smaller than in LiHe. As before, we have set $\alpha = 1$ since the field component perpendicular to the molecular axis is responsible for π state excitation. $\bar{\sigma}_{\text{mol}}^{(2)}$ involves an average over the molecular orientations in the gas target and, accordingly, amounts to $2/3$ of the cross section at $\theta_R = \frac{\pi}{2}$. Besides, the nuclear-motion factor was estimated as $F_{\text{nuc}} \approx 1$ because the transitions mainly occur in a small range of internuclear distances around the equilibrium value.

While the experimental outcome is not reproduced yet, we already see here that the enhancement is much smaller than in LiHe: in a NeHe dimer Γ_a is huge compared to Γ_r and the increase of the branching ratio to essentially 1 cannot compensate for the very strong decrease in the excitation probability caused by a very large broadening of the resonance due to the ICD channel. Therefore, it is this interplay between the photoexcitation and decay steps of 2CPI [see Eq. (10)] which is the key in explaining the counterintuitive result, that the relative enhancement of photoionization due to 2CPI can be much weaker in a relatively small NeHe-system as compared to a large LiHe dimer.

Our description of the experiment on NeHe can be improved by noting that the applied synchrotron beam in [19] had a spectral width of $\Delta\omega = 1.7$ meV which effectively broadens the resonance. At $\min\{\Gamma_a, \Delta\omega\} \gg \Gamma_r$ this effect can be approximately taken into account by the replacement $\Gamma^2 \rightarrow \Gamma_a(\Gamma_a + \Delta\omega)$ in the denominator of Eq. (10). Accordingly, it leads to a damping of 2CPI in NeHe by roughly a factor of $\Gamma_a/(\Gamma_a + \Delta\omega) \approx 0.37$. This reduces the calculated ratio to $\bar{\sigma}_{\text{mol}}^{(2)}/\sigma_{\text{mol}}^{(1)} \simeq 118$, which is to be compared with an approximately 60–100 fold enhancement observed in the experiment [19, 20].

We point out that, from the measured data, a larger ICD width of $\Gamma_a \approx 2$ - 2.5 meV was deduced in [19]. It leads to a somewhat smaller ratio of $\bar{\sigma}_{\text{mol}}^{(2)}/\sigma_{\text{mol}}^{(1)} \approx 76$ - 86.

The above discussion indicates that the spectral width

might have a large detrimental impact on the enhancement effect. However, unlike the ICD width Γ_a , this factor can be avoided by using coherent light sources with very high degree of monochromaticity. Indeed, the feasibility of atomic spectroscopy at $\omega \lesssim 20$ eV and megahertz bandwidths ($\Delta\omega \lesssim 10^{-7}$ eV) has been demonstrated by extending the frequency-comb technique into the extreme ultraviolet domain [32]. Such sources can be employed for an experimental observation of the predicted huge enhancement of photoionization in LiHe.

Conclusion—We have shown that the resonant enhancement of photoionization due to two-center dipole-dipole correlations can be very strongly reduced when the inter-site distance decreases, even though the strength of the correlations *per se* greatly increases. This counterintuitive result also applies to other resonant two-center phenomena, such as, for instance, interatomic photo double ionization [33] and two-center dielectronic recombination [15, 34], which represents the inverse of 2CPI. All this shows that in order to 'extract' most efficiency from the resonant two-center coupling, the latter must not be too strong, i.e., the interacting centers not be located too close to each other.

Acknowledgement

This work has been funded by the Deutsche Forschungsgemeinschaft (DFG, German Research Foundation) under Grant No. 349581371 (MU 3149/4-1 and VO 1278/4-1).

-
- [1] L. S. Cederbaum, J. Zobeley and F. Tarantelli, Phys. Rev. Lett. **79**, 4778 (1997).
 - [2] While the initial state for ICD is usually prepared by photoionization of an inner-valence electron, so-called resonant ICD occurs after photoexcitation; see, e.g., K. Gokhberg, A. B. Trofimov, T. Sommerfeld, and L. S. Cederbaum, Europhys. Lett. **72**, 228 (2005).
 - [3] For reviews on ICD, see U. Hergenhahn, J. Electron Spectrosc. Relat. Phenom. **184**, 78 (2011); V. Averbukh *et al.*, *ibid.* **183**, 36 (2011); T. Jahnke, J. Phys. B **48**, 082001 (2015).
 - [4] S. Marburger, O. Kugeler, U. Hergenhahn, and T. Möller, Phys. Rev. Lett. **90**, 203401 (2003).
 - [5] T. Jahnke *et al.*, Phys. Rev. Lett. **93**, 083002 (2004); Y. Morishita *et al.*, *ibid.* **96**, 243402 (2006); T. Havermeier *et al.*, *ibid.* **104**, 133401 (2010).
 - [6] J. Ullrich, R. Moshhammer, A. Dorn, R. Dörner, L. P. H. Schmidt, and H. Schmidt-Böcking, Rep. Prog. Phys. **66**, 1463-1545 (2003).
 - [7] J. Frenkel, Phys. Rev. **37**, 17 (1931); G. D. Scholes and G. Rumbles, Nature Materials **5**, 683-696 (2006).
 - [8] T. Amthor *et al.*, Phys. Rev. Lett. **98**, 023004 (2007); C. S. E. van Ditzhuijzen, A. F. Koenderink, J. V. Hernandez, F. Robicheaux, L. D. Noordam, and H. B. van

- Linden van den Heuvel, Phys. Rev. Lett. **100**, 243201 (2008).
- [9] T. Jahnke *et al.*, Nature Phys. **6**, 139 (2010); M. Mucke *et al.* **6**, 143 (2010); C. Richter *et al.*, Nat. Commun. **9**, 4988 (2018).
- [10] X. G. Ren, E. L. Wang, A. D. Skitnevskaya, A. B. Trofimov, K. Gokhberg, and A. Dorn, Nat. Physics **14**, 1062 (2018)
- [11] S. Suhai, Phys. Rev. B **51**, 16553 (1995).
- [12] T. Förster, Ann. Phys. (Leipzig) **437**, 55 (1948); T. Renger, V. May and O. Kühn, Phys. Rep. **343**, 137 (2001); E. A. Jares-Erijman and T. M. Jovin, Nature Biotechnol. **21**, 1387 (2003).
- [13] K. Gokhberg, P. Kolorenč, A. I. Kuleff, and L. S. Cederbaum, Nature **505**, 661 (2014).
- [14] B. Najjari, A. B. Voitkiv, and C. Müller, Phys. Rev. Lett. **105** 153002 (2010).
- [15] A. B. Voitkiv and B. Najjari, Phys. Rev. A **82**, 052708 (2010).
- [16] J. Peřina, A. Lukš, V. Peřinová, and W. Leoński, Phys. Rev. A **83**, 053416 (2011); V. Peřinová, A. Lukš, J. Křepelka, and J. Peřina, *ibid.* **90** 033428 (2014).
- [17] A. B. Voitkiv, C. Müller, S. F. Zhang, and X. Ma, New J. Phys. **21**, 103010 (2019)
- [18] F. Grill, A. B. Voitkiv, and C. Müller, submitted (2020) (preprint available on arXiv:2004.02459).
- [19] F. Trinter *et al.*, Phys. Rev. Lett. **111** 233004 (2013).
- [20] G. Jabbari, S. Klaiman, Y.-C. Chiang, F. Trinter, T. Jahnke, and K. Gokhberg, J. Chem. Phys. **140**, 224305 (2014).
- [21] A. Mhamdi *et al.*, Phys. Rev. A **97**, 053407 (2018).
- [22] N. Sisourat, H. Sann, N. V. Kryzhevoi, P. Kolorenč, T. Havermeier, F. Sturm, T. Jahnke, H.-K. Kim, R. Dörner and L. S. Cederbaum, Phys. Rev. Lett. **105**, 173401 (2010).
- [23] A. Hans, P. Schmidt, C. Ozga, C. Richter, H. Otto, X. Holzappel, G. Hartmann, A. Ehresmann, U. Hergenhahn and A. Knie, J. Phys. Chem. Lett. **10**, 1078 (2019).
- [24] Signatures of the nuclear dynamics have also been identified in ICD in He dimers; see T. Havermeier *et al.*, Phys. Rev. Lett. **104**, 133401 (2010); N. Sisourat, N. V. Kryzhevoi, P. Kolorenč, S. Scheit, and L. S. Cederbaum, Phys. Rev. A **82**, 053401 (2010); A. Mhamdi, J. Rist, T. Havermeier, R. Dörner, T. Jahnke, and P. V. Demekhin, Phys. Rev. A **101**, 023404 (2020).
- [25] Since we treat 2CPI in the second order of perturbation theory, the width Γ of the excited state in atom B must be added by 'hand'. When the process is described, instead, within the theory of Fano resonances [15], the excited state automatically receives a non-zero width.
- [26] Note that Eq. (6) contains an effective polarization vector $\mathbf{n}_{\text{eff}} = \mathbf{e}_z - 3 \cos \theta_R \mathbf{e}_R$ which depends on the field polarization and the relative interatomic orientation. It may prove useful for the interpretation of angular emission patterns from 2CPI [21].
- [27] F. Grill, A. B. Voitkiv and C. Müller, Phys. Rev. A **100**, 032702 (2019).
- [28] B. H. Bransden and C. J. Joachain, *Physics of Atoms and Molecules* (Longman Group, Harlow, 1990).
- [29] Atomic spectra database of the National Institute of Standards and Technology (NIST), available at <https://www.nist.gov/pml/atomic-spectra-database>
- [30] B. Friedrich, Physics **6**, 42 (2013).
- [31] The $1s3p$ state in He decays radiatively to the $1s^2$ ($\Gamma_{r,ge}^{(3p)}$) and $1s2s$ states. However, the contribution to $\Gamma_r^{(3p)}$ from the latter is smaller than $\Gamma_{r,ge}^{(3p)}$ by a factor of about 50.
- [32] A. Cingöz, D. C. Yost, T. K. Allison, A. Ruehl, M. E. Fermann, I. Hartl, and J. Ye, Nature **482**, 68 (2012).
- [33] A. C. LaForge, M. Shcherbinin, F. Stienkemeier, R. Richter, R. Moshhammer, T. Pfeifer and M. Mudrich, Nature Phys. **15**, 247 (2019); A. Eckey, A. B. Voitkiv and C. Müller, J. Phys. B **53**, 055001 (2020).
- [34] C. Müller, A. B. Voitkiv, J. R. Crespo Lopez-Urrutia, Z. Harman, Phys. Rev. Lett. **104**, 233202 (2010).